CFD MODELING FOR HELIUM RELEASES IN A PRIVATE GARAGE WITHOUT FORCED VENTILATION

Papanikolaou, E.A. [1] **and Venetsanos, A.G.** [1]
[1] **Environmental Research Laboratory, NCSR Demokritos, Aghia Paraskevi, Attikis, 15310, Greece, e-mail: venets@ipta.demokritos.gr**

ABSTRACT

In the course towards a safe future hydrogen based society, one of the tasks to be considered is the investigation of the conditions under which the use or storage of hydrogen systems inside buildings becomes too dangerous to be accepted. One of the relevant scenarios, which is expected to have a relatively high risk, is a slow (and long lasting) hydrogen release from a vehicle stored in a closed private garage without any forced ventilation, i.e. only with natural ventilation. This scenario has been earlier investigated experimentally (by M. Swain), using He (helium) to simulate the hydrogen behavior. In the present work the CFD code ADREA-HF is used to simulate three of the abovementioned experiments, using the standard k-ε turbulence model. For each case modeled the predicted concentration (by vol.) time series are compared against the experimental at the given sensor locations. In addition the structure of the flow is investigated by presenting the helium concentration field.

NOMENCLATURE

	Upper-case Roman	
P	Pressure	(Pa)
R_i	Specific gas constant of species i	(J kmol^{-1} K^{-1})
T	Temperature	(K)
	Lower-case Roman	
d	Molecular diffusivity of helium to air	(m^2 s^{-1})
g_i	Gravity acceleration in the i-direction	(m s^{-2})
k	Turbulent kinetic energy	(m^2 s^{-2})
q_1, q_2	Mass fraction of component 1, 2	(-)
t	Time	(s)
u_i	i component of velocity	(m s^{-1})
u^+	Normalized parallel to wall velocity	(-)
x_j	Cartesian j co-ordinate	(m)
y^+	Normalized distance from the wall	(-)
y	Distance of current node to nearest solid surface	(m)
z	Cartesian z co-ordinate	(m)
	Lower-case Greek	
ε	Turbulent energy dissipation rate	(m^2 s^{-3})
κ	von Karman constant	(-)
μ, μ_t	Laminar and turbulent viscosity	(kg m^{-1} s^{-1})
ρ, ρ_i	Mixture density, i-component density	(kg m^{-3})
σ	Turbulent Schmidt and Prandtl number	(-)
τ_w	Wall shear stress	(N m^{-2})

1.0 INTRODUCTION

In the course towards a safe future hydrogen based society, one of the tasks to be considered is the investigation of the conditions under which the use or storage of hydrogen systems inside buildings becomes too dangerous to be accepted. The drafting of the associated recommendations/guidelines is today one of the main goals of the HYSAFE project (www.hysafe.org), a goal planned to be implemented through the InsHyDe internal (to HYSAFE) project.

In the past, similar work has been performed for natural gas automotive applications. Grant et al. (1991) [1] examined the hazard assessment of natural gas vehicles in public parking garages, by applying the PHOENICS CFD code. Murphy et al. (1992) [2] examined the extent of indoor flammable plumes resulting from CNG bus fuels system leaks in transit maintenance and storage facilities by applying the FLUENT CFD code.

Refocusing on hydrogen systems, Swain et al. (1998) [3] conducted a large combined experimental-CFD research program, in an effort to determine the ventilation requirements of hydrogen fuelled vehicles' storage in residential garages. The experiments were done with a full-scale model of a single car garage containing a full scale model of a vehicle with simulated leakage of hydrogen (using helium) at a rate of 7,200 Lt/hr. The full-scale garage and vehicle model was built indoors to eliminate the variations of wind and outdoor temperature. The principal question being addressed in this work was, how should existing garages be modified to make them suitable for hydrogen fuelled vehicle storage. The order of preference for garage modifications was modification of garage door without using forced ventilation, modification of garage without using forced ventilation (addition of a passive vent at the garage ceiling) and last modification of garage using forced ventilation and addition of a hydrogen leak detection system. The CFD calculations were performed using FLUENT. Computer modeling done throughout the work showed that the difference in hydrogen and helium concentrations in resembling geometries rarely outgoes 15%. In addition, the largest differences occur during the transient period before steady state and before the highest concentrations are achieved.

Later on Swain et al. (1999) [4] performed hydrogen dispersion experiments in simple vented enclosures and associated CFD validation using the FLUENT code. Recently Agranat et al. (2004) [5] simulated the vented hallway experiment using the PHOENICS code and found results similar to the FLUENT code.

In another work Breitung et al. (2001) [6] applied the GASFLOW CFD code to calculate the temporal and spatial distribution of hydrogen and criteria to evaluate the flame acceleration and detonation potential in an effort to estimate the combustion hazard, due to the boil-off from the cryogenic hydrogen tank of a car in a private garage.

Recently Parsons and Brinckerhoff (2004) [7] evaluated the facility modifications and associated incremental costs that may be necessary to safely accommodate hydrogen fuel cell vehicles in four support facility case studies: commercial multi-story above-ground parking, commercial multi-story below-ground parking, residential two vehicle garages and commercial maintenance/repair/service station. The methodology applied was also CFD.

The above mentioned review of previous work shows that the CFD approach is the commonly applied methodology. On the other hand the specific scenarios considered often include slow flow conditions (laminar or transitional), for which the choice of turbulence model is non trivial. Additional uncertainty can also be introduced by the selection of the grid resolution and the boundary conditions. Clearly there is a need to develop CFD practice guidelines for such kind of flows.

The present work focuses on the abovementioned helium experiments by Swain et al. [3]. Three of these tests were selected for simulation using the ADREA-HF CFD code [8]. The standard k-ε model [9] was selected for turbulence, in order to assess its performance under the specific experimental conditions. For each case modeled the predicted concentrations (by vol.) are compared against the experimental at the given sensor locations. In addition the structure of the flow is investigated by presenting the predicted helium concentration field.

2.0 EXPERIMENTAL DESCRIPTION

Figure 1 shows the geometry of the experimental facility. A full scale single car garage was used. Two vents were installed on the garage door. The first vent location was just at the bottom of the door while the second vent was located at its top. In the experiments different double vent garage door geometries

were tested. In all cases the vents extended the width of the garage door. A full-scale plywood model vehicle (roughly following the dimensions of a Ford Taurus) was placed inside the garage. The wheels were represented by rectangular boxes.

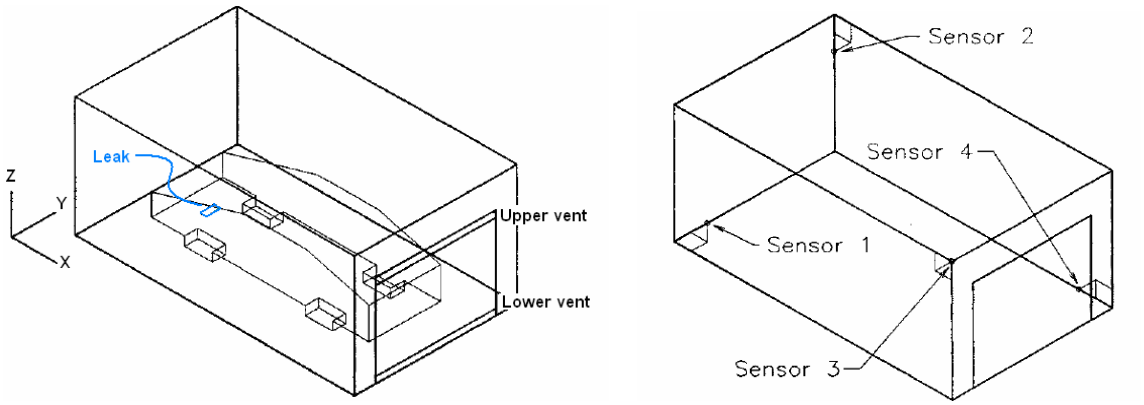

Figure 1. The geometry of the experimental facility (left). The location of the sensors (right)

All testing was done with helium. Helium flow rate was set at 7,200 Lt/hr while its release lasted 2 hours. The leak location was at the bottom of the vehicle and centered at its width. The sensors were located at the four corners of the garage. Figure 1 shows the location of the four sensors. Table 1 lists the geometry dimensions of the experimental facility in SI units.

Table 1. The geometry dimensions of the experimental facility

		X (m)	Y (m)	Z (m)
Garage size		6.4208	3.7084	2.8067
Vehicle location and size (4 wheels, body, chunk and 2 wedges)	Body location	0.7112	1.0414	0.2032
	Body size	4.9784	1.6256	0.60
	Wedge 1 location	0.7112	1.0414	0.8032
	Wedge 1 size	1.60	1.6256	0.543
	Wedge 2 location	4.0896	1.0414	0.8032
	Wedge 2 size	1.60	1.6256	0.543
	Chunk location	2.3112	1.0414	0.8032
	Chunk size	1.7784	1.6256	0.543
	Wheel 1 location	1.350	1.0414	0.00
	Wheel 1 size	0.6096	0.2032	0.2032
	Wheel 2 location	4.40	1.0414	0.00
	Wheel 2 size	0.6096	0.2032	0.2032
	Wheel 3 location	1.350	2.4638	0.00
	Wheel 3 size	0.6096	0.2032	0.2032
	Wheel 4 location	4.40	2.4638	0.00
	Wheel 4 size	0.6096	0.2032	0.2032
Garage door location		6.4008	0.4826	0.00
Garage door size		0.02	2.7432	2.1336
Sensor 1 location		0.3810	0.3810	0.3810
Sensor 2 location		0.3810	3.3274	2.4257
Sensor 3 location		6.0198	0.3810	2.4257
Sensor 4 location		6.0198	3.3274	0.3810
Upper vent location		6.4008	0.4826	1.9558
Upper vent size		0.02	2.7432	Depends on each case
Lower vent location		6.4008	0.4826	0.00
Lower vent size		0.02	2.7432	Depends on each case

Leak location Leak size	1.2 0.1	1.7542 0.2	0.2032 0.00

The following three cases were simulated depending on the height of the vents:

- Case 1: 2.5 inches (6.35 cm) top and 2.5 inches bottom door vents
- Case 2: 9.5 inches (24.13 cm) top and 9.5 inches bottom door vents
- Case 3: 19.5 inches (49.53 cm) top and 19.5 inches bottom door vents

3.0 MATHEMATICAL FORMULATION

The mixing of helium with air was calculated by solving the three dimensional transient, fully compressible conservation equations for mixture mass (continuity equation), mixture momentum (three velocities) and helium mass fraction:

Mixture mass (continuity equation)

$$\frac{\partial \rho}{\partial t} + \frac{\partial \rho u_i}{\partial x_i} = 0 \tag{1}$$

Mixture momentum

$$\frac{\partial \rho u_i}{\partial t} + \frac{\partial \rho u_j u_i}{\partial x_j} = -\frac{\partial P}{\partial x_i} + \rho g_i + \frac{\partial}{\partial x_j}\left((\mu + \mu_t)\left(\frac{\partial u_i}{\partial x_j} + \frac{\partial u_j}{\partial x_i} \right) \right) \tag{2}$$

Helium mass fraction

$$\frac{\partial \rho q_1}{\partial t} + \frac{\partial \rho u_j q_1}{\partial x_j} = \frac{\partial}{\partial x_j}\left(\left(\rho d + \frac{\mu_t}{\sigma} \right) \frac{\partial q_1}{\partial x_j} \right) \tag{3}$$

In the above equations the mixture density is related to component densities (1 for helium and 2 for air) and mass fractions through

$$\frac{1}{\rho} = \frac{q_1}{\rho_1} + \frac{q_2}{\rho_2}; \quad 1 = q_1 + q_2 \tag{4}$$

For the component densities the ideal gas law was assumed valid.

$$P = \rho_i R_i T \tag{5}$$

Turbulence was modeled using the standard k-ε model, in which buoyancy effects were included. In this model turbulent viscosity is calculated from the following equations:

$$\mu_t = C_\mu k^2 / \varepsilon \text{, where } C_\mu = 0.09 \tag{6}$$

The turbulent kinetic energy is obtained from the following transport equation:

$$\frac{\partial \rho k}{\partial t} + \frac{\partial \rho u_j k}{\partial x_j} = \frac{\partial}{\partial x_j}\left(\left(\mu + \frac{\mu_t}{\sigma_k} \right) \frac{\partial k}{\partial x_j} \right) + G + G_B - \rho\varepsilon \text{, where } \sigma_k = 1.0 \tag{7}$$

The volumetric production rate of k by shear forces, G and the buoyancy production (destruction) term, G_B are given by:

$$G = \mu_t \left(\frac{\partial u_i}{\partial x_j} + \frac{\partial u_j}{\partial x_i}\right)\frac{\partial u_i}{\partial x_j} \;\; ; \;\; G_B = -\mu_t \frac{g_z}{\rho\sigma}\frac{\partial \rho}{\partial z} \tag{8}$$

The dissipation rate of the turbulent kinetic energy is obtained from the following transport equation:

$$\frac{\partial \rho\varepsilon}{\partial t} + \frac{\partial \rho u_j \varepsilon}{\partial x_j} = \frac{\partial}{\partial x_j}\left(\left(\mu + \frac{\mu_t}{\sigma_\varepsilon}\right)\frac{\partial \varepsilon}{\partial x_j}\right) + \frac{\varepsilon}{k}\left[C_1\left(G + C_3 G_B\right) - C_2 \rho\varepsilon\right] \tag{9}$$

Where σ_ε, C_1, C_2 and C_3 are constants having values 1.3, 1.44, 1.92, and 1.0 respectively.

Finally the molecular diffusivity of helium to air was taken to be d=5.6494 10^{-5} m^2 s^{-1} as in [4] and the turbulent Schmidt and Prandtl number $\sigma = 0.72$.

4.0 COMPUTATIONAL DOMAIN AND GRID

Given the geometry of the experimental facility and the location of the leak, it was assumed that x-z plane symmetry exists. Therefore, half the width of the geometry was taken into account. Additionally, the computational domain was selected to extend beyond the boundary of the garage, see figure 2. This was done to avoid the uncertainty associated with specification of boundary conditions at the door vents and concentrate more on the assessment of the turbulence model. The present approach clearly requires more computational effort, but is on the other hand the first step towards developing CFD guidelines for vent openings modeling, a task which is left for future work.

The computational grid was Cartesian and its main characteristics are summarized in Table 2. Figure 2 shows the y-z grid for Cases 1, 2, 3 and the x-z grid for Case 1. As can be observed, grid refinement was used close to the door's openings (vents), the source and the walls. The grid becomes coarser as it extends far from the facility. In general the maximum grid expansion ratio was 1.2 while its minimum was 0.84. It can also be observed that the two wedges of the car cut the grid in an irregular manner. This was handled using the porosity formulation, which classifies the cells into fully active (porosity 1), inactive (porosity 0) and partially active (porosity between 0 and 1). The geometrical pre-processing, including the calculation of the porosities was performed using the DELTA-B code [10].

Table 2: The computational grid main characteristics

Case	Grid dimensions	Number of active cells	Min-max cell size in z-dir. (m)	Min-max cell size in x-dir. (m)	Min-max cell size in y-dir. (m)
1	88×26×48	101,887	0.04 close to source 0.5124 m at the top of domain	0.02 close to door 0.92 at the end of domain	0.1 close to source and symmetry plane 0.4011 at the beginning of the domain
2	88×26×50	106,218	0.0381 close to source 0.513 m at the top of domain		
3	88×26×44	93,552	0.0650 m close to the ground 0.5157 m at the top of domain		

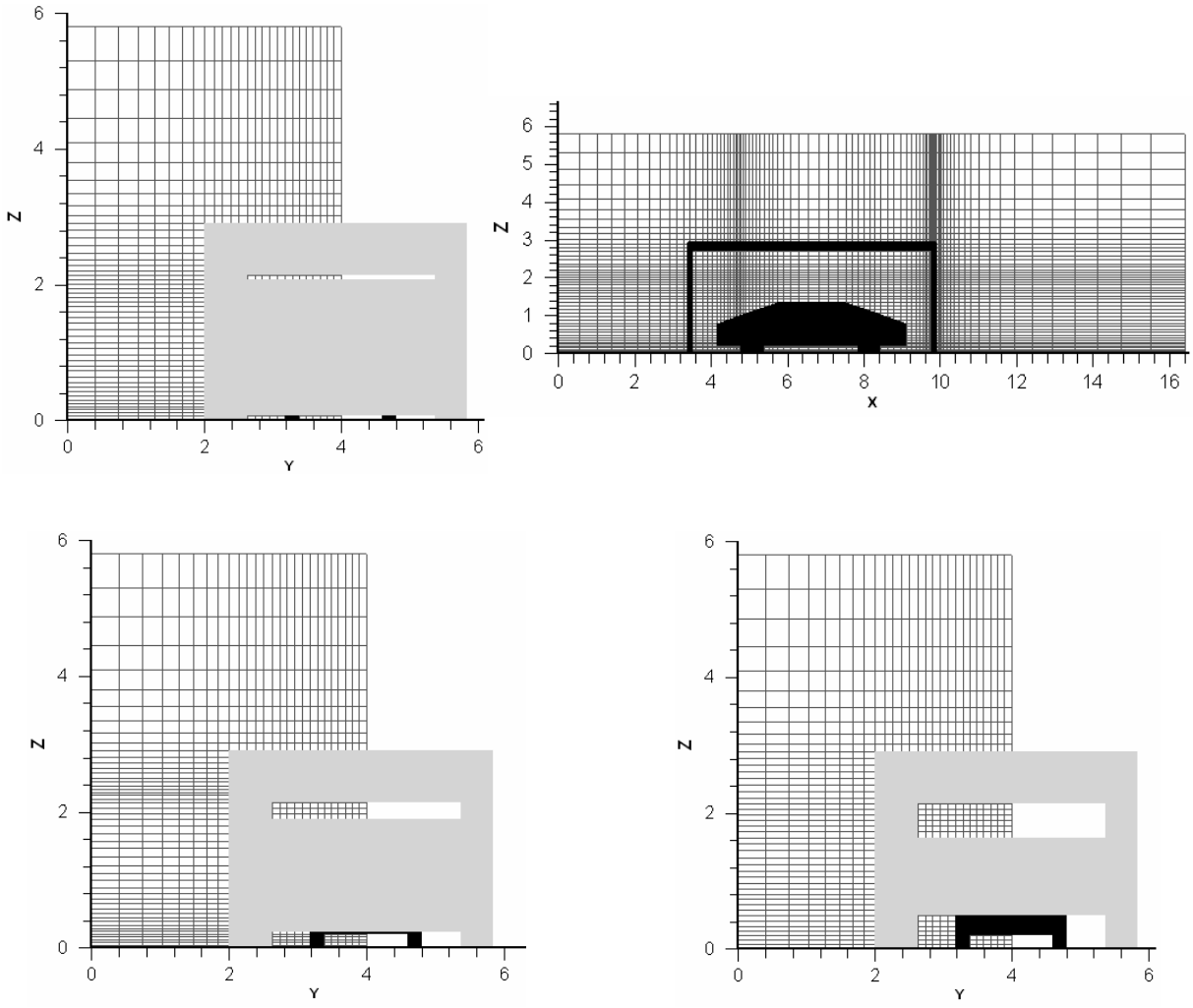

Figure 2. Above: Case 1, below: Case 2 left and Case 3 right

5.0 INITIAL AND BOUNDARY CONDITIONS

Boundary conditions on solid surfaces were zero-gradient for the helium mass fraction while the following wall functions for velocity (parallel to wall component), turbulent kinetic energy and dissipation rate were applied:

$$u^+ = \begin{cases} y^+ & y^+ < 11.6 \\ \frac{1}{\kappa}\ln(9y^+) & y^+ > 11.6 \end{cases}; \qquad k = u_*^2 C_\mu^{-1/2}; \qquad \varepsilon = C_\mu^{3/4}\frac{k^{3/2}}{\kappa y} \tag{10}$$

Symmetry boundary conditions were applied at the symmetry plane, i.e. zero-gradient for all variables except normal velocity, which was set equal to zero.

Inflow boundary conditions were specified at the source, i.e. given velocity (0.1 m s^{-1} normal and 0.0 for other components), helium mass fraction (1.0), pressure (101,325 Pa), turbulent kinetic energy (0.0) and dissipation rate (0.0). Additionally, a zero-gradient was applied for all variables at the source, implying no diffusion across the source surface.

Boundary conditions at the remaining open surfaces of the domain (i.e. except symmetry plane and source) were set as follows: For the normal velocities zero-gradient was assumed at the lateral surfaces. At the top surface normal velocities were obtained from the continuity equation, assuming given constant pressure at the neighboring cells. For the other variables the boundary condition was a function of the flow direction: Zero-gradient was assumed if the flow was directed outwards and given value (equal to the one existing at time 0) was applied when the flow was directed inwards.

Regarding initial conditions, the wind velocity was set to zero, with no turbulence, temperature 293.15 K and hydrostatic pressure.

6.0 NUMERICAL OPTIONS

The ADREA-HF code employs the control volume discretization method, with staggered grid arrangement for the velocities [11]. The first order fully implicit scheme was used for time integration. The first order upwind scheme was used for discretization of the convective terms.

The calculations were performed with an Intel® Xeon™ CPU 3.60GHz with Windows operating system. Figure 3 presents the required CPU times for all three cases. The calculations were performed for a total real time of 7,200 seconds. ADREA-HF has an automatic time step selection mechanism. If the convergence error is above the maximum allowed, the solution is repeated using a smaller time step. In all cases the initial time step was set to 0.001 seconds. In all cases the maximum permitted time step was set to 0.1 seconds. This maximum was reached very early, i.e. within the first 2.8, 1.8 and 1.3 seconds for Cases 1, 2 and 3 respectively and remained constant until the end of the runs. From figure 3 it can be observed that as the vent size increases, the required CPU time slightly decreases.

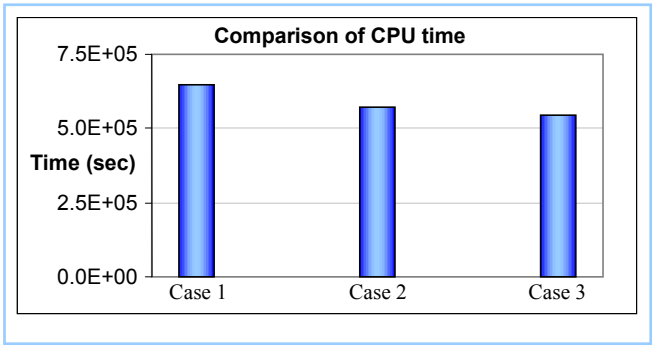

Figure 3. Comparison of CPU times between the three cases

7.0 RESULTS AND DISCUSSION

Figure 4 shows the predicted contours of helium concentration (by vol.) at the symmetry plane at 3,600 seconds from the beginning of the release for Case 1. As can be observed, the vent at the bottom of the door provides a flow of fresh air near the floor, flowing under the vehicle. The vent at the top of the door provides an exit for the low density gas mixture of air and helium, near the ceiling. The use of upper and lower vent produces ventilation that limits the size of the combustible gas cloud to a small portion under the front of the vehicle which extends in the z-direction in front of the vehicle. The rest of the garage gas remained leaner than the lean limit of combustion for H_2. It should be noted that for H_2 the upward propagating lean limit of combustion is 4.1% while its downward propagating lean limit of combustion is 10%. The smallest helium concentration is located near the floor and the door of the garage due to the fresh air inflow from the bottom vent.

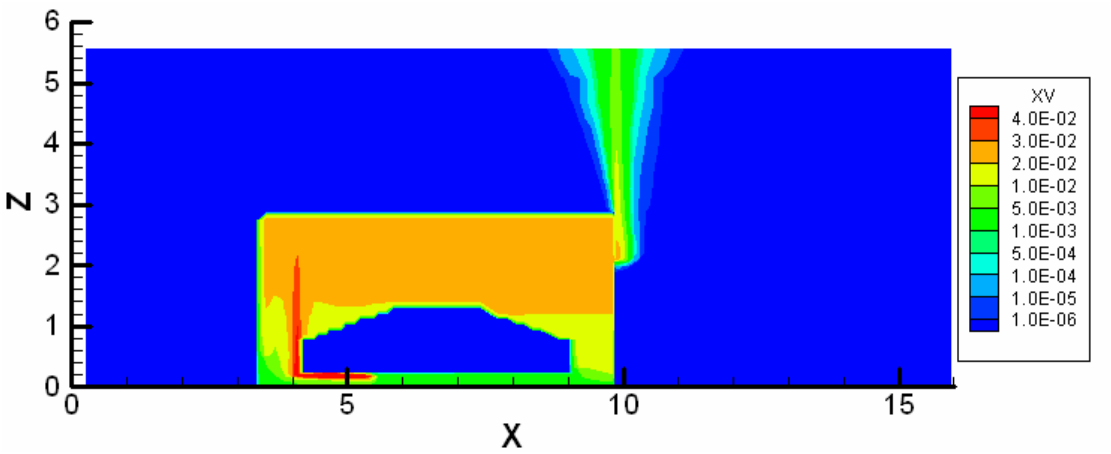

Figure 4: Contours of He concentration (by vol.) at symmetry plane at t=3,600 sec (Case 1)

Figure 5 shows the predicted He concentration versus the measured ones at the four sensor locations for Case 1. As can be seen, the predicted He concentrations agree well with the experimental data for sensors 2 and 3, while there is an overestimation for sensors 1 and 4. The resulting predicted concentration difference between top and lower sensors is underestimated. This could be attributed to the turbulence model overestimating the turbulent mixing.

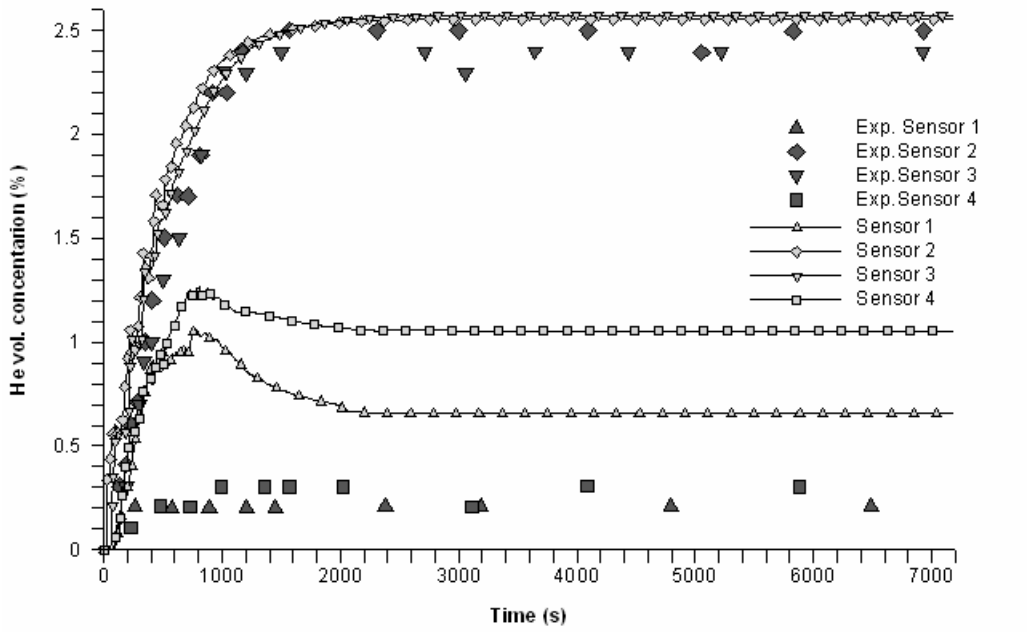

Figure 5. Predicted versus experimental concentrations (by vol.) at the sensor locations (Case 1)

Figure 6 shows the contours of helium concentration in the x-z symmetry plane at 3,600 seconds from the beginning of the release for Case 2. The same observations as in Case 1 can be made for this case too. The dense air entering the bottom vent traveled under the vehicle toward its front. The air replaces the mixture, rich in helium, gas rising from underneath the front of the vehicle. The maximum helium concentration is located near the source while the gas mixture exiting the garage is moving upwards in a column-like shape. Again, the column broadens with height. A comparison between Case 1 and Case 2 shows that the column-like upward moving mixture is broader for Case 2 which means that more mixture gas is leaving the garage in this case. Furthermore, most of the garage gas remained leaner than the lean limit of combustion for H_2 (4.1%) while the increase of the vent size resulted in a combustible cloud from the leak that did not extend far beyond the underside of the front of the

vehicle. It should be noted that now the vent sizes are almost 4 times broader than in Case 1. A comparison of helium volumetric concentration in the x-z symmetry plane at various times after the 3,600 seconds shows that the flow pattern has reached steady state conditions at least at 3,600 seconds.

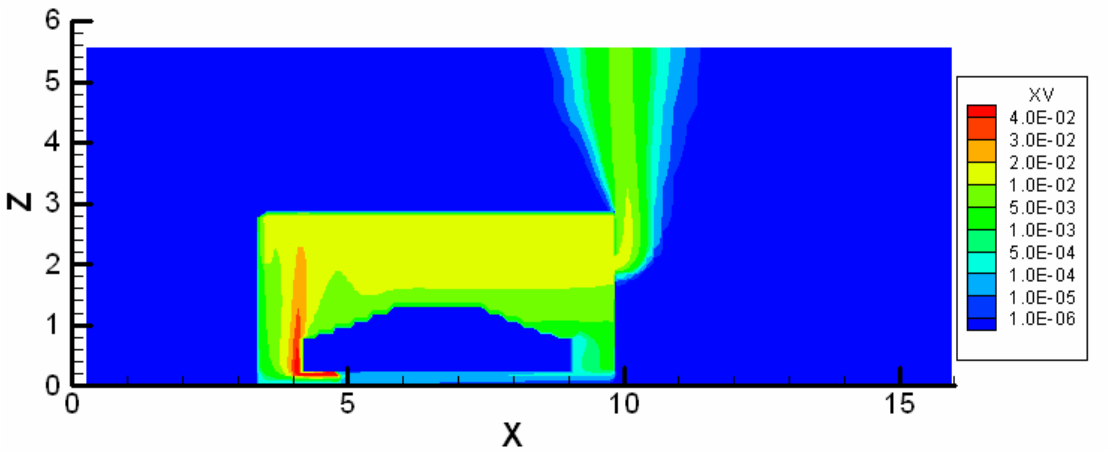

Figure 6. Contours of He concentration (by vol.) at symmetry plane at t=3,600 sec (Case 2)

Figure 7 shows the predicted He concentration versus the measured ones at the four sensor locations for Case 2. As can be observed, the predicted He concentrations are in satisfactory agreement with the experimental data for all sensors. The figure shows a small over prediction for sensors 2, 3 and 4 and a small under prediction for sensor 1.

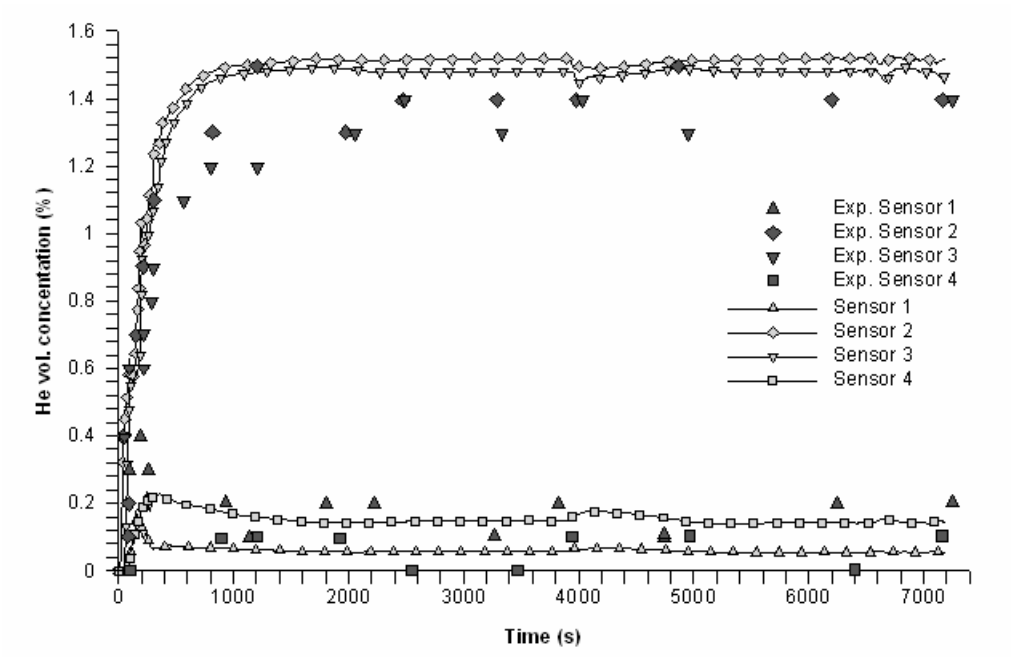

Figure 7. Predicted versus experimental concentrations (by vol.) at the sensor locations (Case 2)

Figure 8 shows the contours of helium concentrations in the x-z symmetry plane at 3,600 seconds from the beginning of the release of the third case. The same observations as in cases 1 and 2 can be made for this case too. A comparison between Figures 4, 6 and 8 shows that as the size of the openings reduces less gas is leaving the garage. The column of the outflow gas is much broader in this case. Consequently, lower helium concentrations exist inside the garage. The maximum helium concentration is located at the source but now it occupies less space. A comparison of helium

volumetric concentration in the x-z symmetry plane at various times after the 3,600 seconds shows that the flow pattern has reached steady state conditions at least at 3,600 seconds.

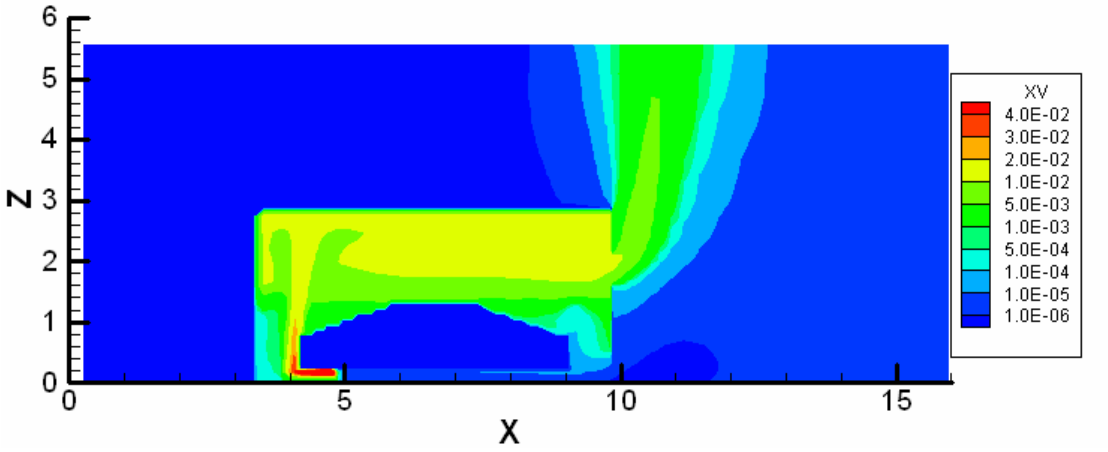

Figure 8. Contours of He concentration (by vol.) at symmetry plane at t=3,600 sec (Case 3)

Figure 9 shows the predicted He concentration versus the measured ones at the four sensor locations for Case 3. As can be observed, the predicted He concentrations are underestimated for sensors 1, 2 and 3. A small over prediction is also observed for sensor 4. Figure 9 suggests that the predicted natural ventilation rate is overestimated.

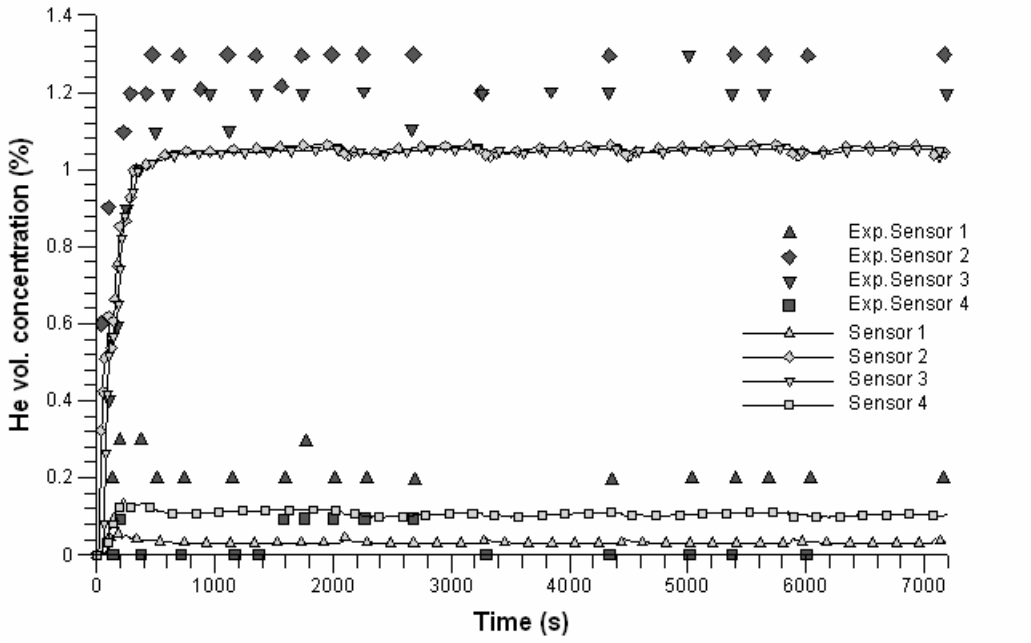

Figure 9. Predicted versus experimental concentrations (by vol.) at the sensor locations (Case 3)

8.0 CONCLUSIONS

The ADREA-HF CFD code was successfully applied to simulate three full scale helium release experiments in a private garage [3], using the standard k-ε turbulence model. The predicted He concentrations (by vol.) time series were compared against the measured ones at the four experimental sensor locations. The predicted results were found generally in acceptable agreement with the experiment. For the case with the lowest vent size the vertical concentration gradient was found

underestimated compared to the experiment. This was attributed to the turbulence model overestimating mixing under the given low flow conditions. Additionally, the calculations revealed the mixing patterns and showed that the mixing mechanisms reached a near-equilibrium state resulting in a constant cloud size and shape during the release period. Finally, the performed calculations underline the importance of applying the CFD methodology to evaluate the potential hazards especially under complex release conditions.

9.0 ACKNOWLEDGEMENTS

The authors would like to thank the Greek Secretariat of Research and Technology as well as the European Commission for funding of this work through the 02-PRAKSE-42 and HYSAFE-NoE projects respectively.

10.0 REFERENCES

1. Grant, T.J., Shaaban, S.H. and Zalak, V.M., Hazard assessment of natural gas vehicles in public parking garages, Final Report, work performed by Ebasco Services Inc. for the Brooklyn Union Gas Company, 1991.
2. Murphy, M.J., Brown, S.T. and D.B. Philips, Extent of indoor flammable plumes resulting from CNG bus fuels system leaks, International Truck and Bus meeting and exposition, Toledo, Ohio, US, November 16-19, 1992 (SAE technical paper No 922486).
3. Swain, M.R., Grilliot, E. S. and M.N. Swain, Phase 2: Risks in indoor vehicle storage, in Addendum to Hydrogen Vehicle Safety Report: Residential Garage Safety Assessment, analysis conducted by: Michael R. Swain, University of Miami, under subcontract to Directed Technologies Inc, prepared for the Ford motor company under prime Contract No. DE-AC02-94CE50389 to the U.S. Department of Energy, Office of Transportation Technologies, August 1998
4. Swain, M.R., Grilliot, E. S. and M.N. Swain: Experimental verification of a hydrogen risk assessment method, Chemical Health and Safety, 1999, pp. 28-32.
5. Agranat, V., Cheng, Z. and Tchouvelev, A., CFD Modeling of Hydrogen Releases and Dispersion in Hydrogen Energy Station, Proceeding of WHEC-15, 2004, Yokohama.
6. Breitung, W., Necker, G., Kaup, B. and Veser, A., Numerical simulation of hydrogen in a private garage, Proceedings of the fourth international symposium on hydrogen power–theoretical and engineering solutions–Hypothesis IV, Stralsund (Germany), 9-14 September 2001.
7. Support facilities for hydrogen fuelled vehicles-Conceptual design and cost analysis study, Technical report, 2004, Prepared for California Fuel Cell Partnership by Parsons and Brinckerhoff in association with TIAX and University of Miami.
8. Bartzis, J. G., ADREA-HF: A three dimensional finite volume code for vapour cloud dispersion in complex terrain, EUR report 13580 EN, 1991
9. Launder, B. E. and Spalding, D. B., The numerical computation of turbulent flow, *Computer Methods in Applied Mechanics and Engineering*, **3**, Issue 2, pp. 269-289
10. Venetsanos, A. G., Catsaros, N., Würtz, J. and Bartzis, J. G., The DELTA_B code. A computer code for the simulation of the geometry of three-dimensional buildings. Code structure and users manual, EUR report 16326 EN.
11. Patankar, S. V., Numerical heat transfer and fluid flow, 1980, Hemisphere Publishing Corporation.